

CO₂-BRINE INJECTIVITY TESTS IN HIGH CO₂ CONTENT CARBONATE FIELD, SARAWAK BASIN, OFFSHORE EAST MALAYSIA

A Giwelli¹, MZ Kashim², MB Clennell¹, L Esteban¹, R Noble¹, C White¹, S Vialle³, M Ghasemiziarani³, M Myers¹, A Saeedi³, S Salwani Md Shah²

¹CSIRO, Australia,

²PETRONAS Research Sdn Bhd, Malaysia

³Curtin University

This paper was prepared for presentation at the International Symposium of the Society of Core Analysts held in Trondheim, Norway, 27-30 August 2018

ABSTRACT

We conducted relatively long duration core-flooding tests on three representative core samples under reservoir conditions to quantify the potential impact of flow rates on fines production/permeability change. Supercritical CO₂ was injected cyclically with incremental increases in flow rate (2–14 ml/min) with live brine until a total of 7 cycles were completed. To avoid unwanted fluid-rock reaction when live brine was injected into the sample, and to mimic the in-situ geochemical conditions of the reservoir, a packed column was installed on the inflow accumulator line to pre-equilibrate the fluid before entering the core sample. The change in the gas porosity and permeability of the tested plug samples due to different mechanisms (dissolution and/or precipitation) that may occur during scCO₂/live brine injection was investigated. Nuclear magnetic resonance (NMR) T₂ determination, X-ray CT scans and chemical analyses of the produced brine were also conducted. Results of pre- and post-test analyses (poroperm, NMR, X-ray CT) showed no clear evidence of formation damage even after long testing cycles and only minor or no dissolution (after large injected pore volumes (PVs) ~ 200). The critical flow rates (if there is one) were higher than the maximum rates applied. Chemical analyses of the core effluent showed that the rock samples for which a pre-column was installed do not experience carbonate dissolution.

INTRODUCTION

Carbon capture and storage (CCS) has been identified as transformative technologies to achieve deep reductions in CO₂ emissions specified under the Kyoto Protocol. Geological storage has been a major attractive options for CO₂ disposal owing to its reasonable capacity, secure and longer retention times and technical feasibility¹. Among all the elements that qualify geological media as viable storage options, injectivity is one of the key parameters that determine the success of CO₂ storage in field operations. CCS project operators seek to sequester large amounts of CO₂ into subsurface reservoirs using a minimum number of wells to minimize costs and to reduce leakage risks. Therefore,

within the constraint of maximum allowable wellhead pressure limits, a high injection rate is often desired. However, this might prompt injectivity-related problems due to: salting-out effects at the near-bore region due to brine vaporization by injected CO₂²⁻⁵, multiphase-flow effects^{6, 7} and scale/fines formation and mobilization caused by geochemical effects and mechanical dragging⁸. To date, no study has been reported investigating the injectivity issues for highly heterogeneous and complex carbonate fields, though there are some studies that have been conducted on parameterizing CO₂ injectivity in carbonates⁹⁻¹².

In this study, we aimed to evaluate the effect of supercritical CO₂ (scCO₂) flow rates on fines production/permeability change and particle mobilization caused by geochemical effects, which might occur during storage operations in a carbonate gas field with approximately 70% CO₂ content (called A field) located in East Malaysia's waters. CO₂ injection has been planned for the aquifer zone which is highly saturated with dissolved CO₂ due to the high CO₂ partial pressure. scCO₂ was injected cyclically in a number of increments (2–14 ml/min) with live brine flooding until a total of 7 cycles were completed. Furthermore, to avoid unwanted geochemical reactions (dissolution and/or precipitation) when the live brine flows into the samples and to mimic deep reservoir conditions, a mineral-packed column (based on the calcite and dolomite percentage mineralogy of the cores) was developed and installed upstream of the core.

In addition to the main coreflood experiments, a number of auxiliary diagnostic measurements were conducted on pre-and post-flood samples, i.e., gas porosity and permeability, NMR T₂ and X-ray CT imaging, to better understand dissolution and/or precipitation mechanism that could occur during scCO₂/live brine injection. Furthermore, core effluents during scCO₂ injection (2-14 ml/min) were collected for ICP (Inductively Coupled Plasma) analysis.

EXPERIMENTAL MEASUREMENTS AND PROCEDURES

Experimental Apparatus

A three-phase, steady-state core-flooding apparatus was used to carry out the injectivity experiments¹³. A schematic of the core-flooding apparatus used in this study¹⁴ is shown in Figure 1.

The apparatus is designed for pressures up to 15,000 psi (1,000 bar) and temperatures up to 200°C in one stand-alone integrated system. More information about the apparatus, data logging and monitoring/controlling system is provided in Saeedi¹⁵. The core-holder, fluid accumulators and flow-lines carrying the fluids are located in a convection oven with three fans to keep the temperature constant during the experiments (with an accuracy of +/- 0.2°C).

As mentioned earlier, a calcite-dolomite packed column was installed on the inflow accumulator line immediately before fluid enters the core-samples (highlighted in red in

Figure 1). The column, made with thick walled 1 inch outer diameter corrosion resistant alloy tubing, was made with the correct proportion of calcite and dolomite grains, as per reservoir mineralogy provided by PETRONAS. The column length is 30.5 cm and total volume of the packed sediment in the tube was 48.7cm³.

Core Samples and Brine Composition

Three carbonate core samples were chosen from aquifer zone in the A field. Mineralogy of the samples indicates the rock composition was dominated by 44% calcite and 54% dolomite and sporadic quartz (1%) and clay (1%). Table 1 shows the pre-test properties of the core samples.

Live brine was prepared in a high pressure-high temperature stirred Parr reactor using high purity CO₂ (99.99 wt%) and a synthetically prepared formation water (SFW). Base salinity of the composition (pre-flood) was 21,056 mg/L. Table 2 shows major ions composition of SFW generated at CSIRO's laboratory in comparison with formation brine provided by PETRONAS. React program (Geochemist's Workbench® Version 8.0) was used to ensure the salts remain soluble at P-T reservoir conditions (Table 3) used in these experiments. The model shows high concentration of HCO₃ at ambient condition might cause some precipitates during brine preparation, and thus we decided to reduce bicarbonate concentration (HCO₃) to 400 mg/l (see Table 2), avoiding incompatibility issue during brine preparation.

Experimental Protocol

Details for the other auxiliary diagnostic measurements (listed above) conducted pre- and post-flood samples are given below.

X-ray CT imaging was used to check the degree of heterogeneity inside each sample as well as the potential changes to the core-scale and, to some extent, the pore-scale features in each sample due to the flooding procedure. In this study, all scan procedures on the samples (pre- and post- test) were performed at room temperature and atmospheric pressure using an X-ray energy beam of 140 kV and 1500 mA. A helical acquisition mode (pitch at 350 µm) was used to enable the reconstruction of 3D X-ray images with a voxel size of about 110 µm × 110 µm × 400 µm (DICOM 2D images format with 512 × 512 pixels).

The plug samples were then vacuum saturated¹⁶ in SFW using a pressure saturator at a pressure of approximately 2000 psi for 48 hours. To assist the saturation, a vacuum pump was used limited to around 30 mins to prevent water evaporation which would increase the brine salinity¹⁶. The liquid pore volume is calculated from gravimetric measurements before and after saturation. NMR measurements were collected, on this fully brine-saturated, using Oxford-GIT Instruments Geospec 2 Plus Analyzer. The NMR acquisition that were used parameters are provided in Table 4.

For every coreflood experiment, the fully SFW saturated core-sample was wrapped in Teflon tape to prevent the rough surface of the rock from damaging successive layers. The sample was then inserted into heat-shrink sleeve which was then heated using a heating gun to shrink into position and anchor the sample and any spacers in line with it. The sample was then wrapped in aluminium tape to provide an impermeable barrier such that CO₂ could not migrate into the confining sleeve (to prevent the high likelihood of supercritical CO₂ explosive decompression related damage) and then inserted into a Viton sleeve while placed on the core-holder's inlet end plug (Figure 2). The sleeve dimensions are engineered to perfectly fit the outer diameter of the plugs while leaving a small annular space between the outer diameter of the sleeve and the inner diameter of the core-holder. The assembly was then inserted into the core-holder body and the inlet end cap was screwed into place. In order to minimise the effect of gravity segregation during coreflood experiments, the fluid was injected vertically (bottom to top) with pretty high rates. An overburden pressure was applied using a syringe-type pump and care was taken not to increase the overburden pressure above the desired reservoir net effective pressure. This was achieved by increasing the confining pressure in stages, with each stage having the pore pressure also increased in order to keep the net overburden pressure similar to the reservoir condition. It should be mentioned that the temperature inside the oven where the fluid bottles, separator, the core-holder and the collection pumps' reservoirs are located, was maintained at ~150°C.

After the desired in-situ reservoir conditions were reached (see Table 3), pre-equilibrated live brine (fluid passed through the packed column, except sample 17-012) was injected at 1 ml/min to displace dead brine. Then cyclic scCO₂- brine flooding was injected until a total of 7 cycles were completed for each tested sample. scCO₂ injection rate was increased in a number of increments (2 - 14 ml/min) to examine the effect of flow rates on fines production/permeability change, i.e., the minimum flow rate at which small particles detach and migrate within the pores of the formation¹⁷⁻²¹. Then the CO₂ injection rate was returned to 2 ml/min (except 17-012) after each incremental stage of high flow rate in order to calculate any permeability impairment in the Darcy flow region. Live brine was injected at a constant rate of 1 ml/min to displace scCO₂ (imbibition). A simplified diagram of the applied cyclic floods is illustrated in Figure 3.

The core effluents were collected for ICP (Inductively Coupled Plasma) analysis. It is worth nothing that we were not able to collect effluents from the packed column, before the fluids entered the core sample, during the experiments. Due to fluid sample bottles capacity, we decided to inject an average of 25 pore volume each cycle (total injected PV of ~ 200) before we switched the pumps. For some cycles, differential pressure fluctuation was observed even after a long period of injection.

At the completion of each experiment, confining pressure and pore pressure were released gradually and the core sample was removed from the core-holder. After unloading the sample, it was placed in a vented oven to dry at 80°C so it could undergo the post-flood characterisation (gas porosity, gas permeability and XCT). It should be

mentioned that no salt cleaning process was performed after flooding as the expected amount of salt in the pore volume is $< 2\%$. Finally, the tested samples were re-saturated with SFW for the post-test NMR T_2 measurement.

RESULTS AND DISCUSSION

Figures 4a&b show an example of differential pressures (Δp) during cyclic CO_2 - brine flooding for 17-012 (without the packed column) and 17-016 (with the packed column). Fluctuations in the scCO_2 differential pressure during the first few cycles were observed, and these decreased as the scCO_2 flow rate increased. These fluctuations are likely due to either the difficulty associated with low flow rate operation of back-pressure regulators during two-phase flow or due to small scale dissolution or/and precipitation. Higher scCO_2 flow rates seem to displace more live brine, as the end-effect becomes less pronounced. As mentioned above, some cycles showed differential pressure fluctuation even after a long period of injection (~ 25 pore volumes passed through the core); this could be as a result of CO_2 bubble/clusters trapped in the pore space which put a strain on the brine flow.

Figures 4c-e show differential pressure response at different scCO_2 injection rates throughout the test. Darcy's law was obeyed over the time averaged measurement even when flow was unstable over the short term. It should be mentioned that samples 17-011 & 17-016 showed around $\pm 5\%$ deviation from the regression line and this could be attributed to differential pressure fluctuation during the first cycles of the test (Figures 4a&b).

Effective brine and scCO_2 permeabilities were calculated using Darcy's law (shown in Fig. 5). Please note that injection rates were kept at 1ml/min (imbibition tests) for brine and 2 ml/min (drainage tests) for scCO_2 (except 17-012 where the scCO_2 injection rate did not return to 2 ml/min after each incremental stage) during all the tested cycles. Result shows scCO_2 permeabilities change was relatively minimal at a given saturation (except 17-011 where the back-pressure regulator was unstable at 10 ml/min until the end of the test). On the other hand, brine permeabilities for 17-011 & 17-016 show substantial decrease, which might be expected from k_{rw} as saturation decreases with higher scCO_2 injection rate. During imbibition phase, a fraction of CO_2 will become disconnected and immobile and thus, it is not possible to drive all of the CO_2 out of the pores. Brine permeability of 17-012 shows unusual values that could be due to high scCO_2 rates used prior the imbibition cycles (scCO_2 rate did not return to 2 ml/min after each incremental rate as in 17-011 & 17-016).

As mentioned earlier, core effluents were collected during scCO_2 injection (2-14 ml/min). The result of calcium mobilisation in the three plugs is shown in Figure 6. Results are adjusted with respect to the base brine composition, so any positive number is a net increase in dissolution. Sample 17-012 was compared with 17-011 and 17-016 to understand the effectiveness of the packed column (pre-treated live brine) to reduce dissolution (Figure 6). Clearly, 17-012 was much more reactive than the other two

samples. Unfortunately, due to technical limitation during the experiments, we were not able to collect post-packed column effluents (before the fluids entered the core sample) to compare with the injected FSW composition. Therefore, further experiments will be needed to clarify the effect of the packed column on brine composition.

As stated above, dimensions, gas porosity and gas permeability of the tested samples were measured before subjecting them to the flooding procedure. These measurements were repeated again on the post-flood samples. Table 1 summarises the results of these measurements. Sample 17-012 (without the packed column) shows porosity enhancement of about 7.8%, while 17-011 & 17-06 (with the packed column) show porosity reduction of 0.4 & 0.9%, respectively. The porosity enhancement in 17-012 could be due to dissolution reaction we observed in Figure 6. Permeability, on the other hand, has slightly decreased for all the tested samples and the change ranged from 2.2 to 5.4%. Such alterations are the results of one or several mechanisms such as mineral precipitation, possible fines migration released by mineral dissolution in the inlet face and/or mechanical compaction.

X-Ray CT Scan Imaging

X-ray CT images were generated for all the tested samples before and after flooding at ambient conditions. CT imaging was used to qualitatively (due to low signal to noise ratio from the subtraction between pre- and post-XCT images) analyse possible spatial changes of the bulk density along the plug axis and directly threshold pores in 3D due to possible simultaneous mechanisms (e.g. dissolution, precipitation and/or compaction) which might occur during flooding experiments. The CT-value profile computed from transversal x-ray images (every 400 μm along the plug axis) was converted into an apparent dry bulk density profile from calibration with standard solid minerals (Figure 7). The CT profile of 17-012 (without packed column) shows lower CT number/bulk density than would be suggested from either dissolution reactions or damage, while 17-016, where the live brine was pre-treated in the packed column, shows negligible CT number/bulk density changes after flooding (within the CT scan resolution $> 0.1 \text{ mm}$). Furthermore, 3D X-ray CT pre- and post-flooding images (Figure 8) were generated for the core samples and shows some low-density areas (corresponding to a light grey colour) due to voids (i.e. cracks and pores).

Nuclear Magnetic Resonance (NMR)

NMR measurements were conducted on all samples twice at 100% brine saturation; pre (blue line) and post-test (red line), and an example is shown in Figure 9. The NMR T_2 relaxation times recorded are used to calculate the connected porosity filled by brine and demonstrate (qualitatively) the pore size distribution of brine saturated samples. The T_2 value of a single pore is proportional to the surface-to-volume ratio of the pore, which is directly related to the porosity and pore size distribution of the rock, scaled according to surface relaxation strength, normally considered to be constant for a particular rock-fluid pair²². Results indicate a decrease in the amount of large pore sizes, i.e., decrease of the

intensity of the long T_2 centred near 500 ms and evolution of new smaller pores centred near 40 ms. This observation suggests two possible scenarios: (i) dissolution mechanism occurred in small pores and precipitation mechanism in some of the large pores, (ii) fines dislodgement from smaller pores which could clog pore throat access to large pores.

CONCLUSION

We examined the effect of $scCO_2$ flow rates on fines production/permeability change by looking for the minimum flow rate at which small particles detach and migrate within the pores of the formation. The change in the petrophysical properties of the core samples due to different mechanisms (dissolution, precipitation, and mechanical compaction) that may occur during $scCO_2$ /live brine injection was investigated. The occurrence and intensity of these mechanisms was evaluated using non-destructive observation techniques conducted on the tested core samples (NMR, X-ray CT-scan, gas porosity, and gas permeability) and also the chemical analysis of the produced brine. Based on the data and information gathered from the measurements and analysis conducted the following conclusions can be drawn:

1. No clear evidence of formation damage (reduction or enhancement in permeability) occurred for the selected core samples, when flooded at high rates with the potential to move fine particles.
2. If there is a critical flow rate (CFR) for the onset of formation damage, it is higher than the maximum achievable laboratory flow rates for the presented samples.
3. Within the resolution of the CT scan machine, we observed minor (at inlet face) to no dissolution; a small level of pore enlargement was noted but this did not penetrate into the sample more than a few mm (except 17-012, where we did not use pre-treated CO_2 -saturated brine) even after large injected pore volumes of approximately 200.

ACKNOWLEDGEMENTS

The authors would like to acknowledge financial support from PETRONAS.

REFERENCES

1. IPCC. Special Report on Carbon Dioxide Capture and Storage. In: Metz, B., Davidson, O., de Coninck, H.C., Loos, M., Meyer, L.A. (Eds.). Cambridge University Press, Cambridge, UK and New York, NY, USA, Chapter 5, pp. 195–276. 2005.
2. Muller N, Qi R, Mackie E, Pruess K, Blunt MJ, "CO₂ injection impairment due to halite precipitation," *Greenhouse Gas Control Technologies*, (2009) **1**, 3507-14.
3. Pruess K, & Muller N, "Formation dry-out from CO₂ injection into saline aquifers: Part 1, Effects of solids precipitation and their mitigation," *Internal Report- Lawrence Berkeley National Laboratory*, <http://escholarship.org/uc/item/9p44q7x3>, (2009)
4. Ott H, Roels SM, de Kloe K, "Salt precipitation due to supercritical gas injection: I. Capillary-driven flow in unimodal sandstone," *Int J Greenh Gas Control*, (2015) **43**, 247-55.

5. Jeddizahed J, & Rostami B, "Experimental investigation of injectivity alteration due to salt precipitation during CO₂ sequestration in saline aquifers," *Advances in Water Resources*, (2016) **96**, 23-33.
6. Svec RK , & Grigg RB. "Physical effects of WAG fluids on carbonate core plugs. SPE-71496-MS," In *SPE Annual Technical Conference and Exhibition* New Orleans, Louisiana 30 September-3 October, 2001.
7. Mohamed IM, & Nasr-El-Din HA, "Fluid/Rock Interactions During CO₂ Sequestration in Deep Saline Carbonate Aquifers: Laboratory and Modeling Studies," *SPE Journal*, (2013) **18**, 468-85.
8. Xie Q, Saeedi A, Delle Piane C, Esteban L, Brady PV, "Fines migration during CO₂ injection: Experimental results interpreted using surface forces," *Int J Greenh Gas Control*, (2017) **65**, 32-9.
9. Izgec O, Demiral B, Bertin HJ, Akin S. "Experimental and numerical modeling of direct injection of CO₂ into carbonate formations. SPE-100809-MS," In *SPE Annual Technical Conference and Exhibition*, San Antonio, Texas, USA, 24-27 September, 2006.
10. Mohamed IM, He J, Nasr-El-Din HA. "Permeability change during CO₂ injection in carbonate rock: A coreflood study. SPE-140943," In *SPE Production and Operations Symposium*, Oklahoma city, Oklahoma, March 27-29, 2011.
11. El Hajj H, Odi U, Gupta A. "Carbonate reservoir interaction with supercritical carbon dioxide," In *International Petroleum Technology Conference*, Beijing, China 26-28 March, 2013.
12. Khather M, Saeedi A, Rezaee R, Noble RRP, Gray D, "Experimental investigation of changes in petrophysical properties during CO₂ injection into dolomite-rich rocks," *Int J Greenh Gas Control*, (2017) **59**, 74-90.
13. Saeedi A, Rezaee R, Evans B, Clennell B, "Multiphase flow behaviour during CO₂ geo-sequestration: Emphasis on the effect of cyclic CO₂-brine flooding," *J Petrol Sci Eng*, (2011) **79**, 65-85.
14. Khather M, Saeedi A, Rezaee R, Noble RRP, "Experimental evaluation of carbonated brine-limestone interactions under reservoir conditions-emphasis on the effect of core scale heterogeneities," *Int J Greenh Gas Control*, (2018) **68**, 128-45.
15. Saeedi A. *Experimental study of multiphase flow in porous media during CO₂ geo-sequestration processes*, Springer Theses. Recognizing outstanding Ph.D Research, Kensington, (2012),
16. McPhee C, Reed J, Zubizarreta I. *Core Analysis: A Best Practice Guide*, Elsevier (2015), 852.
17. Gabriel GA, & Inamdar GR. "An experimental investigation of fines migration in porous media, SPE-12168-MS," In *SPE Annual Technical Conference and Exhibition*, San Francisco, California, 5-8 October, 1983.
18. Amaerule JO, Kersey DG, Norman DK, Shannon PM "Advances in formation damage assessment and control strategies, PETSOC-88-39-65," In *Annual Technical Meeting*, Calgary, Alberta, 12-16 June, 1988.

19. Leone AL, & Scott EM "Characterization and control of formation damage during waterflooding of a high-clay-content reservoir," *SPE Reservoir Engineering Journal*, (1988) 1279-86.
20. Miranda RM, & Underdown DR. "Laboratory measurement of critical rate: A novel approach for quantifying fines migration problems, SPE-25432," In *Annual Technical Conference and Exhibition*, Oklahoma, 21-23 March, 1993.
21. Hassani A, Mortazavi SA, Gholinezhad J, "A new practical method for determination of critical flow rate in Fahliyan carbonate reservoir," *J Petrol Sci Eng*, (2014) **115**, 50-6.
22. Coates GR, Xiao L , Prammer MG. *NMR logging principles and applications*, Halliburton Energy Services, Division of Halliburton Co Houston, United States, (1999), 234.

Table 1. Pre- and post-test values of the core samples used in the study

Sample ID#	17-011		17-012		17-016	
	Pre-test	Post-test	Pre-test	Post-test	Pre-test	Post-test
Length (cm)	6.650		7.136		5.567	
Diameter (cm)	3.750		3.750		3.812	
Gas porosity (%)	27.0	26.9	27.0	29.1	22.6	22.4
Gas permeability (mD)	27.7	27.1	29.7	28.1	13.3	13.0

Table 2. Concentration of major ions of formation brine and synthetic brine prepared at CSIRO laboratory

Major ions	Formation water (mg/l)	SFW (mg/l)
Calcium, Ca	246	247
Magnesium, Mg	47	46
Potassium, K	311	311
Sodium, Na	7653	7653
Strontium, Sr	73	73
Bicarbonate, HCO ₃	2140	400
Chlorite, Cl	12348	12348

Table 3. Experimental P-T conditions

Reservoir parameter	value
Pore pressure (psi)	5250
Net confining pressure (psi)	1390
Reservoir temperature (°C)	150
CO ₂ partial pressure (psi)	3500

Table 4. NMR acquisition parameters used during the NMR measurements

Recycle delay (ms)	SNR	Number of echoes	Tau (ms)	Number of point per echo
7500	100	43860	1000	1

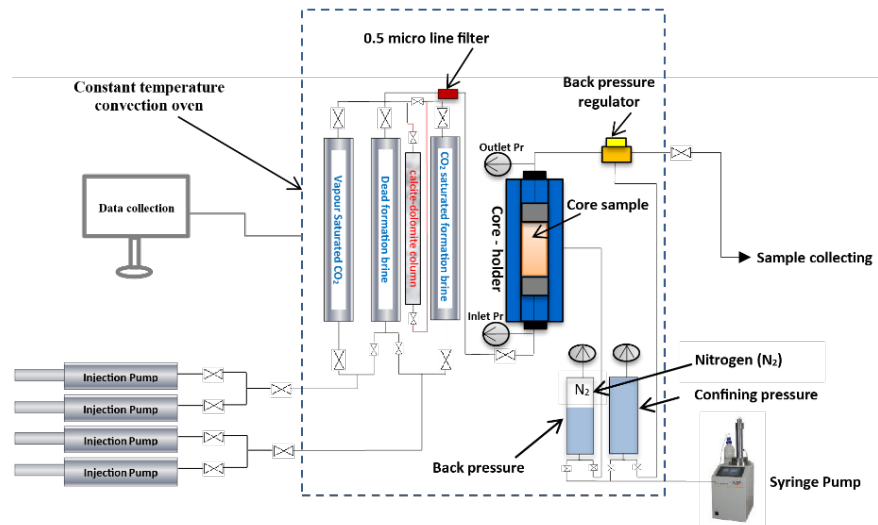


Figure 1. Schematic diagram of coreflooding apparatus used in this study ¹⁴

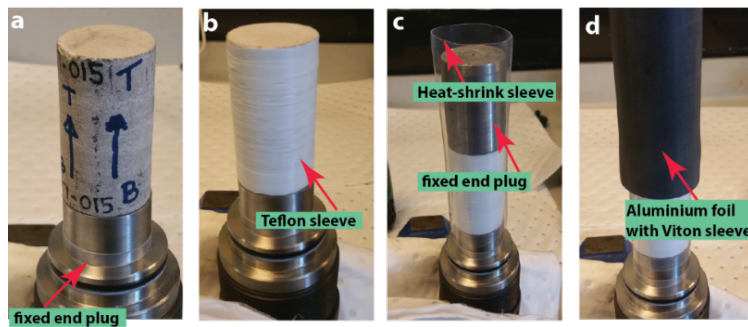


Figure 2. An example of core-sample preparation and assembly for coreflooding experiment

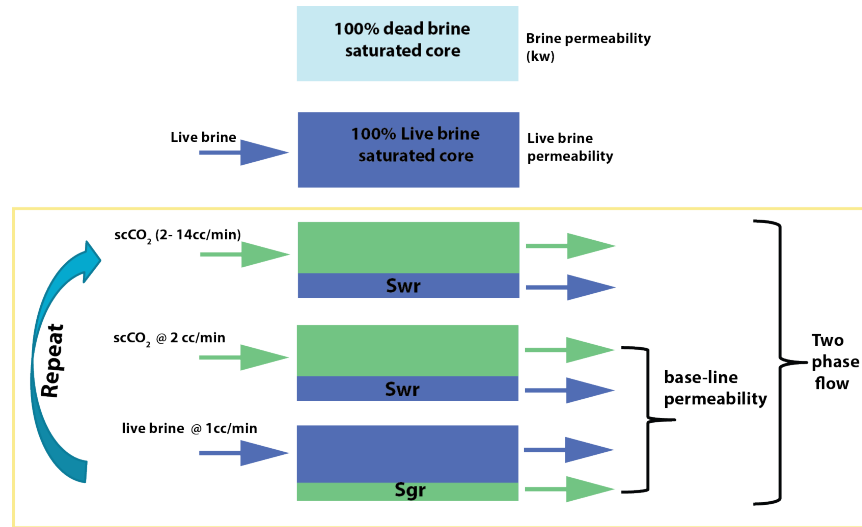


Figure 3. Schematic of the protocol used for this study

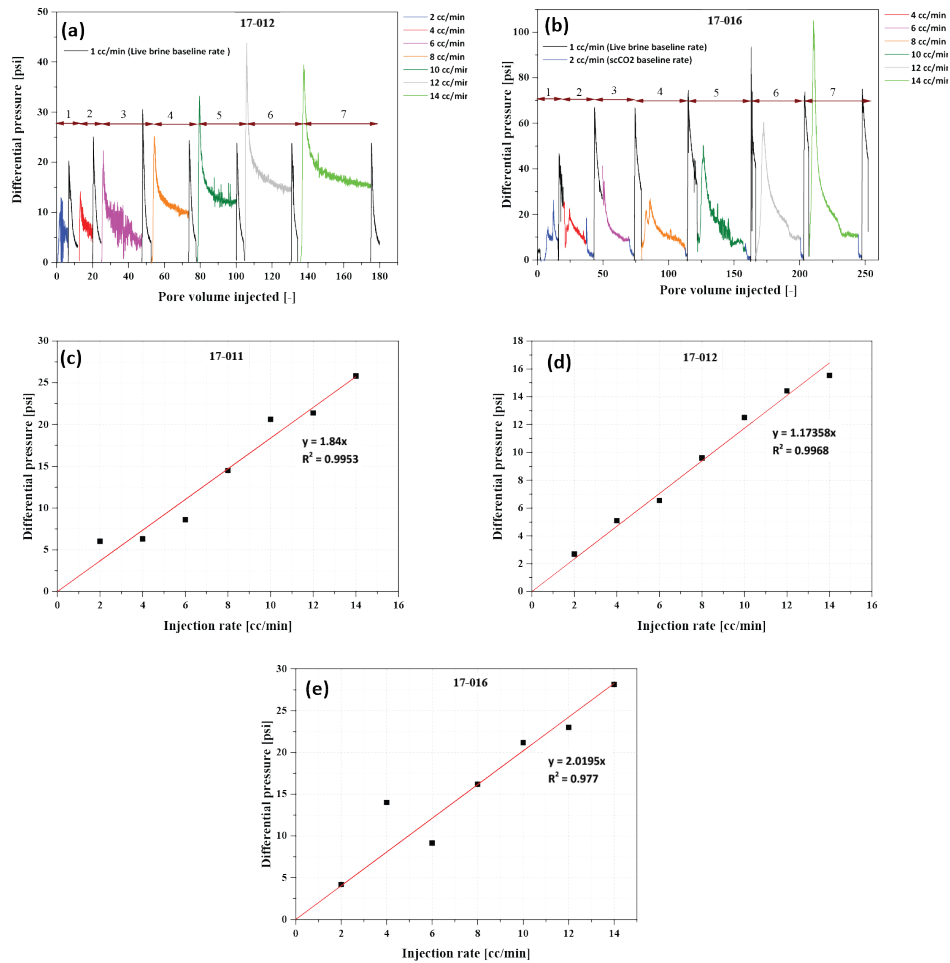


Figure 4. (a) & (b) differential pressure evolution across 17-012 & 17-016 during cyclic CO₂-brine flooding. Live brine (black line) and scCO₂ (blue line) base flow rates were constant throughout the test, and (c-e) shows scCO₂ differential pressures response vs flow rates. Darcy's law was obeyed

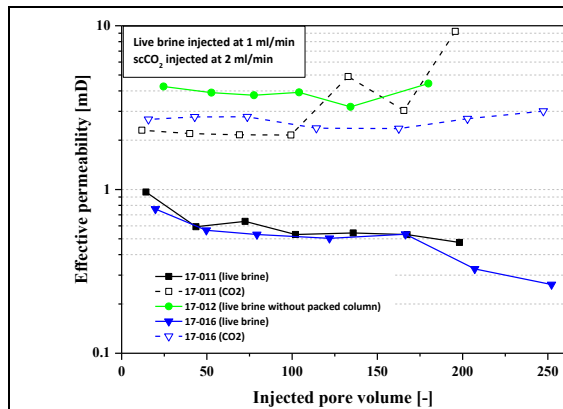


Figure 5. Effective brine and scCO_2 permeabilities calculated using Darcy's law. Live brine was injected at 1 ml/min and scCO_2 was injected at 2 ml/min during all the cycles. Please note that scCO_2 permeability at 2 ml/min was not measured for 17-012

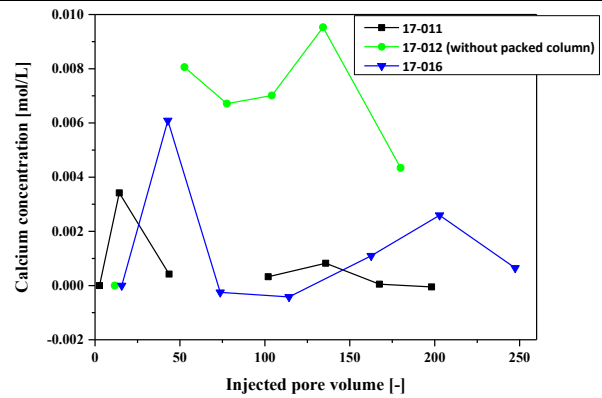


Figure 6. Calcium concentration in the core effluents collected during scCO_2 injection for the flooded plugs. Calcium mobility was adjusted for background brine composition for all the plugs

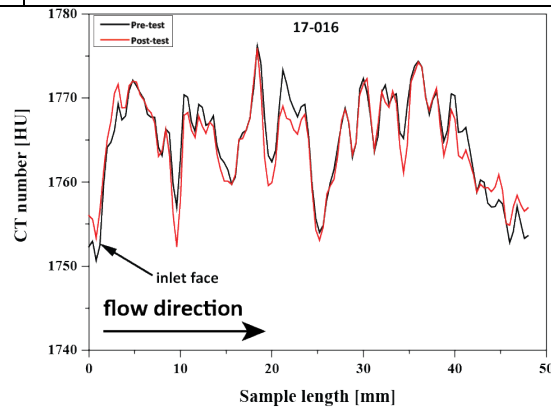
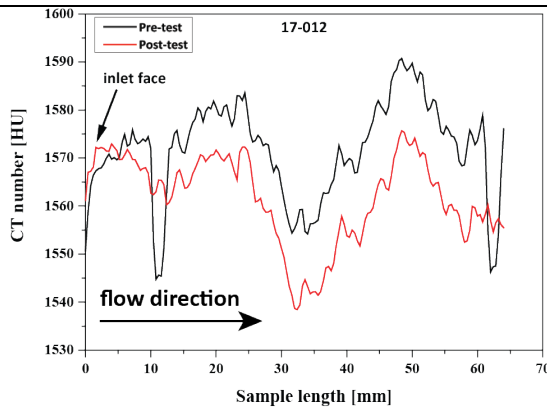


Figure 7. CT value distribution before and after flooding. The CT number profiles show obvious signs of dissolution in 17-012 (without the packed column) while 17-016 (with the packed column) shows no visible dissolution reaction along the plug at the XCT resolution (> 0.1 mm)

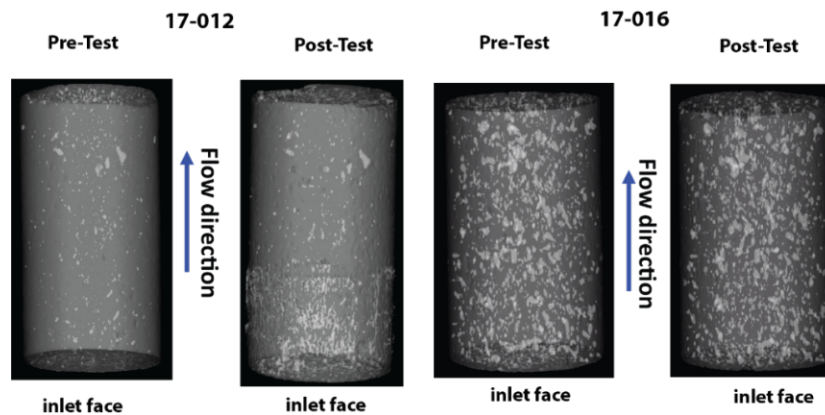


Figure 8. 2D view of x-ray images of both 17-012 and 17-016

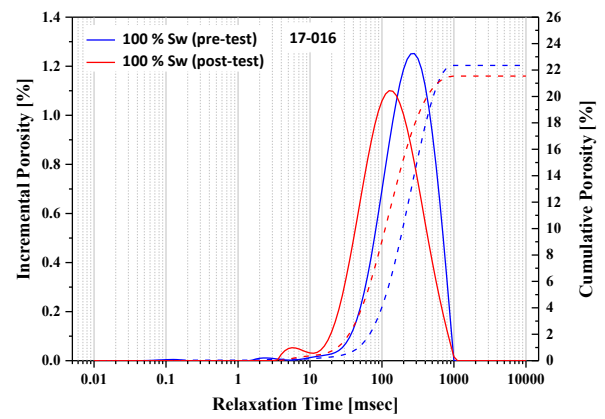


Figure 9. Change in the incremental and cumulative NMR T_2 distribution of 17-016 before and after flooding